

Characterization and reactivities of transient species generated by laser flash photolysis of *N*-hydroxypyridine-4-thione

PERKIN
2

Maksudul M. Alam,^a Osamu Ito,^{*a} Günther N. Grimm^b and Waldemar Adam^b

^a Institute for Chemical Reaction Science, Tohoku University, Katahira, Aoba-ku, Sendai 980-8577, Japan

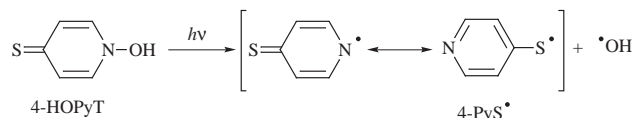
^b Institute of Organic Chemistry, University of Würzburg, Am Hubland, D-97074 Würzburg, Germany

Received (in Cambridge) 16th June 1998, Accepted 27th August 1998

The reaction intermediates produced by the nanosecond-laser-flash photolysis of *N*-hydroxypyridine-4-thione (4-HOPyT) have been studied in aqueous and nonaqueous solutions. The pyridyl-4-thiyl radical (4-PyS[•] at 420 nm) and [•]OH are formed by the homolytic N–OH bond cleavage of 4-HOPyT. The 720-nm band was assigned to the pyridyl-*N*-oxyl radical (4-S=PyO[•]) generated by the photodissociation of the O–H bond and by H abstraction from 4-HOPyT through [•]OH. The triplet state of 4-HOPyT [³(4-HOPyT)*], confirmed by energy transfer with triplet quenchers, is also produced concomitantly with the radical species. Diffusion controlled electron-transfer reactions occur between ³(4-HOPyT)* and donors (or acceptors), which may be caused by the relatively high triplet-state energy ($E_T = 60.1 \text{ kcal mol}^{-1}$) of ³(4-HOPyT)*. In aqueous alkaline solution, the solvated electron (e_{aq}^-) and the one-electron semioxidized radical of 4-HOPyT (4-S=PyO[•]) are produced by photoionization of the anionic form of 4-HOPyT. Thus, it is possible to control the generation of [•]OH and e_{aq}^- by changing the pH of the solution.

Introduction

Thiols, sulfides and disulfides with pyridine moieties have been widely recognized as useful chemical reagents for synthetic purposes (Barton's reagents).^{1–6} Furthermore, since *N*-hydroxypyridinethiones (HOPyT's) are known as biologically active compounds with antifungal, antibacterial and anticancer properties,^{7–10} their zinc and sodium salts have been used commercially in antidandruff shampoos.¹¹ Moreover, HOPyT's are capable of producing hydroxyl radical upon photolysis (Scheme 1),^{6,12–17} which has special importance as a cytotoxic agent in



mouse cells and Chinese hamster fibroblasts, but only in the presence of light.^{14,17} For this purpose, laser flash photolysis is particularly effective for the detection of reactive intermediates such as triplet states and radicals.^{15–18}

In the present study, we have applied the nanosecond-laser photolysis method to reveal the reactive species produced from *N*-hydroxypyridine-4-thione (4-HOPyT), which is known to be predominantly present as the thione form in tautomeric equilibrium with the minor thiol form in solution.¹⁹ Thus, it is also necessary to clarify the nature of the intermediates formed by either N–O or O–H bond cleavage. 4-HOPyT also exhibits an acid–base equilibrium ($pK_a = 3.82$).¹⁹ In particular it would be expected that pH changes could alter the transient species generated from 4-HOPyT. Furthermore, some MO calculations were performed to rationalize the experimental results.

Results and discussion

Steady-state absorption spectra

The UV–visible absorption spectrum of 4-HOPyT in THF (Fig. 1) shows intense absorption peaks at 300 nm ($\epsilon = 9400$

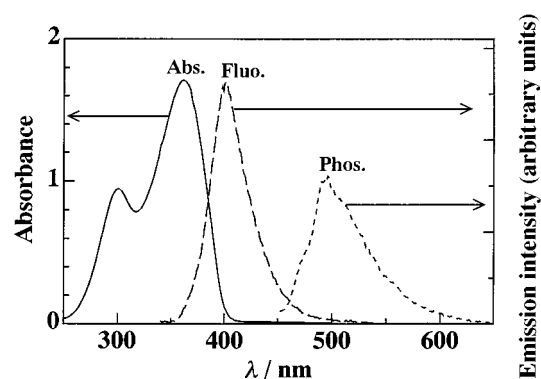


Fig. 1 Steady UV–VIS (—) and fluorescence (---, $\lambda_{exc} = 362 \text{ nm}$) spectra of 4-HOPyT ($0.1 \times 10^{-3} \text{ mol dm}^{-3}$) in THF (1.0-cm optical path); phosphorescence spectrum (-----, $\lambda_{exc} = 362 \text{ nm}$) of 4-HOPyT in glassy frozen Me-THF at 77 K.

$\text{mol}^{-1} \text{ dm}^3 \text{ cm}^{-1}$) and 362 nm ($\epsilon = 17\,000 \text{ mol}^{-1} \text{ dm}^3 \text{ cm}^{-1}$), which suggests that both the 300- and 362-nm bands are characteristic $^1(\pi-\pi^*)$ transitions of the C=S chromophore of thiones.^{18,20–23} The fluorescence and phosphorescence spectra of 4-HOPyT are also shown in Fig. 1, which may be emitted from the 362 nm band of 4-HOPyT. The absorption spectral shape of the dilute 4-HOPyT solution ($0.05 \times 10^{-3} \text{ mol dm}^{-3}$) is the same as that of the concentrated solution (up to $1.0 \times 10^{-3} \text{ mol dm}^{-3}$). The absorption intensities increase proportionally with concentration and follow the Beer–Lambert law, which indicates insignificant aggregation of 4-HOPyT in the concentration range $0.05\text{--}1.0 \times 10^{-3} \text{ mol dm}^{-3}$.¹⁸

Transient spectra in organic solvents

The transient absorption spectra of the laser flash photolysis of 4-HOPyT ($0.4 \times 10^{-3} \text{ mol dm}^{-3}$) at 355 nm in Ar-saturated THF exhibit two absorption bands at 420 and 720 nm with a shoulder at 680 nm, as shown in Fig. 2. The absorption intensity of the 420-nm band decreases with a fast and a slow decay component (see inset of Fig. 2), which indicates the formation

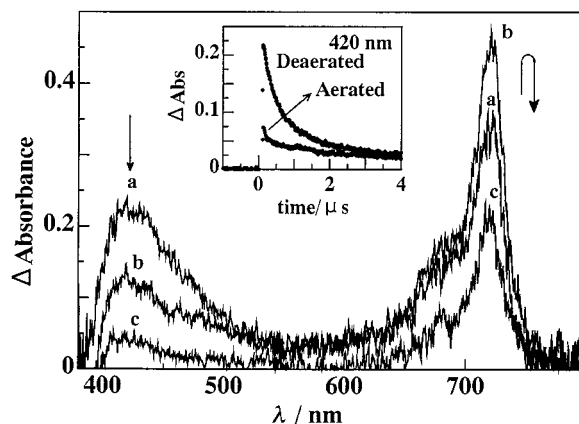
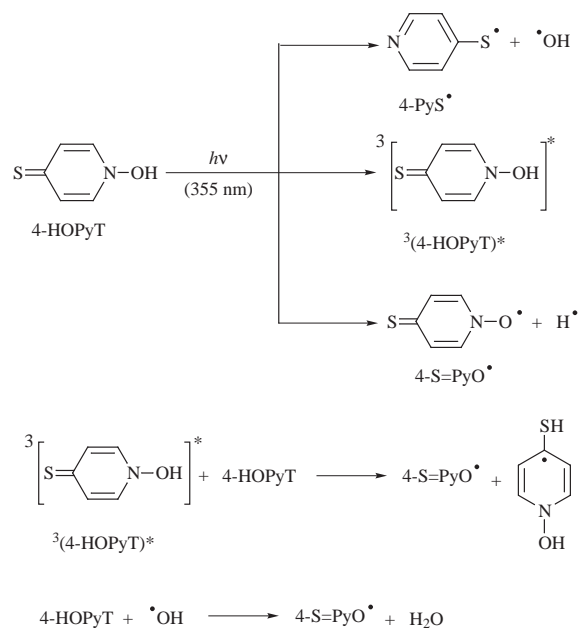


Fig. 2 Transient absorption spectra observed after laser photolysis of 4-HOPyT ($0.4 \times 10^{-3} \text{ mol dm}^{-3}$) at 355-nm excitation in Ar-saturated THF (detector, MCPD); (a) 50 ns, (b) 350 ns and (c) 2000 ns. Inset: time profiles of the 420-nm absorption band (detector, PMT).

of two different transient species. The fast decay component was efficiently quenched by O_2 (see inset in Fig. 2) and other triplet quenchers such as ferrocene and β -carotene, which suggests that the 420-nm band can be attributed to triplet-triplet absorption of $^3(4\text{-HOPyT})^*$.^{16,18,23} The triplet lifetime (τ_T°) was evaluated as 2.8 μs from the decay of the 420-nm transient band at low laser power (2–3 mJ pulse^{-1}) and in very dilute THF solution of 4-HOPyT using the equation $1/\tau_T = 1/\tau_T^\circ + k_{\text{sq}}[4\text{-HOPyT}]$.^{18,23}

The rate of the slow decay part (see inset in Fig. 2) was not affected by the presence of triplet quenchers such as O_2 and β -carotene. Thus, the slow decay component is attributed to the pyridinyl-4-thiyl radical (4-PyS $^\bullet$), which was produced concomitantly with $^3(4\text{-HOPyT})^*$, followed by the homolytic N–OH bond fission of 4-HOPyT to afford $^\bullet\text{OH}$ (Scheme 2) as



Scheme 2

reported in recent studies.^{14–17} A similar transient absorption band to 4-PyS $^\bullet$ appeared at 420 nm by homolytic photodissociation of the S–S bond of 4,4'-dipyridine disulfide (DPDS) in Ar-saturated THF [eqn. (1)],^{15,16,24} which also confirms the generation of 4-PyS $^\bullet$ from 4-HOPyT (Scheme 2). Since the decay rate of the 4-PyS $^\bullet$ absorption (420-nm band) was not affected by O_2 , this species shows a low reactivity towards O_2 , which is one of the characteristics of such arylthiyl radicals.^{15,16,24,25} The

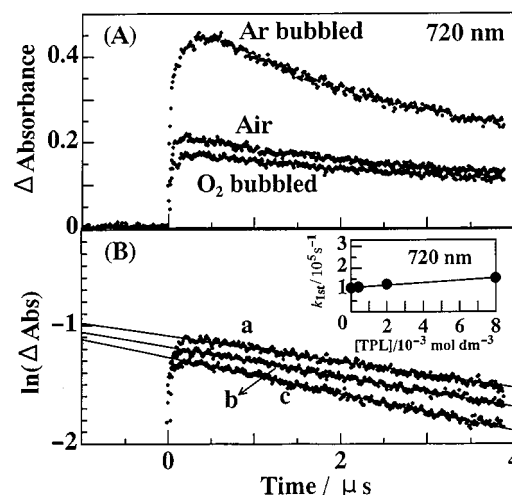
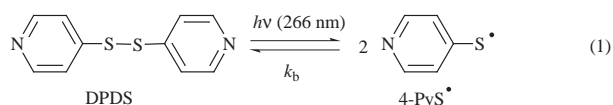


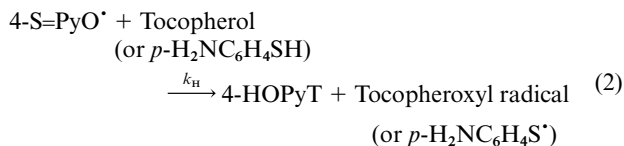
Fig. 3 (A) Time profiles of the 720-nm absorption band of 4-HOPyT ($0.4 \times 10^{-3} \text{ mol dm}^{-3}$) in 355-nm laser photolysis in Ar-saturated THF and (B) first-order rate plots in the presence of tocopherol; [tocopherol] (a) 0.0, (b) 2.0×10^{-3} and (c) $8.0 \times 10^{-3} \text{ mol dm}^{-3}$ (detector, PMT). Inset: pseudo-first-order plot for the hydrogen-abstraction reaction.



decay of 4-PyS $^\bullet$ is attributed to recombination to the disulfide, as presumed from the second-order plot.^{15,16,24}

In contrast, the absorption bands at 720 and 680 nm appeared immediately after the laser pulse; afterwards their absorption intensities rose for ca. 1 μs and then decayed (Fig. 2). The rise in the intensity was quenched by O_2 (Fig. 3A) and other triplet quenchers, which suggests that the secondary reaction of $^3(4\text{-HOPyT})^*$ with 4-HOPyT (Scheme 2) is responsible for this slow rise. The initial main absorption intensities of the 720- and 680-nm bands, which appeared immediately after the laser pulse, were not affected by triplet quenchers such as O_2 and β -carotene. Thus, the 720- and 680-nm bands may be assigned to an O-centered radical (4-S=PyO $^\bullet$), which is produced by direct O–H bond cleavage as well as by H-abstraction from the ground state 4-HOPyT by the reactive $^3(4\text{-HOPyT})^*$ and by $^\bullet\text{OH}$ (Scheme 2). The absorption maxima of 4-S=PyO $^\bullet$ in the longer wavelength region support the assigned quinoid structure.

Slow hydrogen abstraction by the 720- and 680-nm species (Fig. 3B) from α -tocopherol (or aminobenzenethiol) to generate the tocopheroxyl radical at 420 nm¹⁸ (or the aminobenzenethiyl radical at 480 nm)¹⁸ was observed [eqn. (2)] with



the rate constant $k_{\text{H}} = 5.6 \pm 0.8 \times 10^6 \text{ mol}^{-1} \text{ dm}^3 \text{ s}^{-1}$ (or $5.8 \pm 0.8 \times 10^7 \text{ mol}^{-1} \text{ dm}^3 \text{ s}^{-1}$). These H-abstraction reactions are expected for 4-S=PyO $^\bullet$. The $^\bullet\text{OH}$ may also be important for H-abstraction from α -tocopherol.

Triplet quenching rate constants

From the increase in the decay rates of $^3(4\text{-HOPyT})^*$ at 420 nm in the presence of O_2 , the second-order triplet-quenching rate constant [k_{O_2} in eqn. 3)] was evaluated as $2.7 \pm 0.14 \times 10^9 \text{ mol}^{-1}$

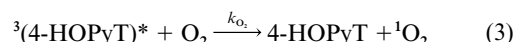


Table 1 Rate constants for the energy transfer (k_{ent}) of $^3(4\text{-HOPyT})^*$ to triplet quenchers at 23 °C in Ar-saturated THF

Quenchers	$E_{\text{T}}/\text{kcal mol}^{-1}$	$k_{\text{ent}}/\text{mol}^{-1} \text{ dm}^3 \text{ s}^{-1 a}$
β -Carotene	19.4 ^b	3.9×10^9
O ₂	22.5 ^c	2.7×10^9
Ferrocene	42.9 ^d	2.5×10^9
Anthracene	42.7 ^c	3.1×10^9
1,3-CHD ^e	52.4 ^c	1.1×10^9
Benzil	54.3 ^c	9.6×10^7

^a Estimated error is $\pm 5\%$ of the stated values. ^b Ref. 27(c). ^c Refs. 18 and 27(a). ^d Ref. 27(b). ^e CHD is cyclohexa-1,3-diene.

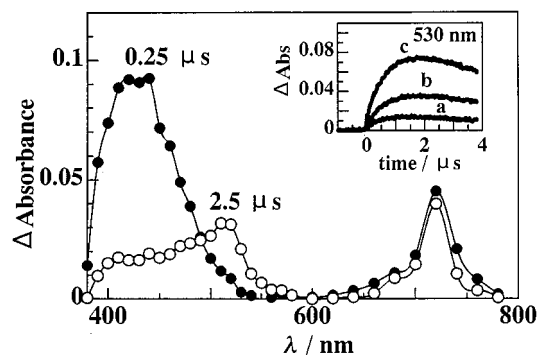
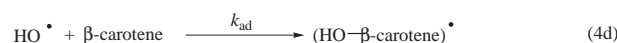


Fig. 4 Transient spectra of the laser photolysis of 4-HOPyT ($0.2 \times 10^{-3} \text{ mol dm}^{-3}$) in the presence of β -carotene ($0.05 \times 10^{-3} \text{ mol dm}^{-3}$) at 355-nm excitation in Ar-saturated THF (detector, PMT). Inset: rise of $^3(\beta\text{-carotene})^*$ at 530 nm; [β -carotene] (a) 0.025, (b) 0.05 and (c) $0.075 \times 10^{-3} \text{ mol dm}^{-3}$.

$\text{dm}^3 \text{ s}^{-1}$ in THF. The formation of singlet oxygen was confirmed by the consumption of 1,3-diphenylisobenzofuran (DPBF).^{18,26}

Fig. 4 shows the transient spectra of $^3(4\text{-HOPyT})^*$ in the presence of β -carotene in Ar-saturated THF. A new absorption band was observed at 530 nm, while the 420-nm absorption of $^3(4\text{-HOPyT})^*$ decreased. The absorption band at 530 nm (see inset in Fig. 4) is attributed to the T-T absorption band of β -carotene [$^3(\beta\text{-carotene})^*$],¹⁸ which indicates energy transfer from $^3(4\text{-HOPyT})^*$ to β -carotene [eqn. (4a)].¹⁸ The competitive addition reactions of $\cdot\text{OH}$, $^3(4\text{-HOPyT})^*$ and 4-PyS^* to the double bonds of β -carotene [eqn. (4b–4d)]^{16,24} may cause the



low intensities of the absorption bands of $^3(\beta\text{-carotene})^*$ and 4-S=PyO^* at 530 and 720 nm, respectively.

The rate constant [k_{ent} in eqn. (4a), Table 1] for energy transfer from $^3(4\text{-HOPyT})^*$ to β -carotene was evaluated from the slopes of the pseudo-first-order plots of the first-order rate constants ($k_{1\text{st}}$) obtained by curve fitting with a single exponential of the rise curve of $^3(\beta\text{-carotene})^*$ at 530 nm. For other triplet quenchers, the k_{ent} values are summarized in Table 1. Although the k_{ent} value for cyclohexa-1,3-diene ($1.1 \times 10^9 \text{ mol}^{-1} \text{ dm}^3 \text{ s}^{-1}$; $E_{\text{T}} = 52.4 \text{ kcal mol}^{-1}$)^{18,27} is close to the diffusion controlled limit ($k_{\text{d}} = 1.2 \times 10^{10} \text{ mol}^{-1} \text{ dm}^3 \text{ s}^{-1}$ in THF),²⁴ the k_{ent} value for benzil ($9.6 \times 10^7 \text{ mol}^{-1} \text{ dm}^3 \text{ s}^{-1}$; $E_{\text{T}} = 54.3 \text{ kcal mol}^{-1}$)^{18,27} is about 1/100 of k_{d} , which indicates that E_{T} of $^3(4\text{-HOPyT})^*$ is *ca.* 57.3 kcal mol⁻¹, as calculated from the Sandros equation.²⁸

The lowest triplet energy (E_{T}) of $^3(4\text{-HOPyT})^*$ was also calculated from the 0–0 transition of the phosphorescence band at 475 nm, which was measured in glassy Me-THF at 77 K (Fig. 1)

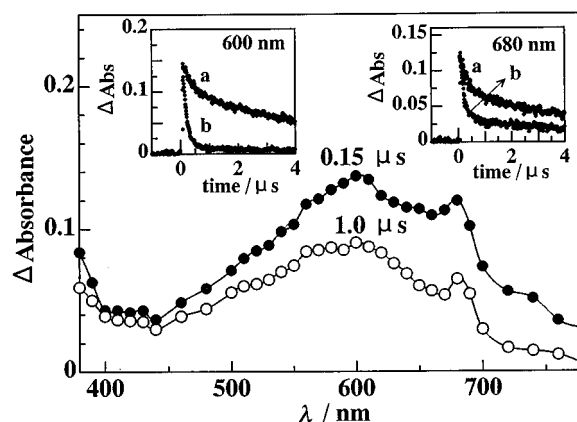
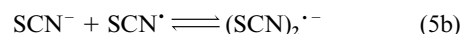


Fig. 5 Transient absorption spectra in the laser photolysis of 4-HOPyT ($0.2 \times 10^{-3} \text{ mol dm}^{-3}$) at 355-nm excitation in Ar-saturated aqueous alkaline (pH 12) solution (detector, PMT). Inset: decay time profiles in (a) Ar-saturated and (b) O₂-saturated solutions.

to be $60.1 \pm 0.2 \text{ kcal mol}^{-1}$. This is in agreement within *ca.* 2.5 kcal mol⁻¹ with the E_{T} value determined by quenching experiments of $^3(4\text{-HOPyT})^*$. In ethanol glass at 77 K, the phosphorescence peak is shifted to shorter wavelength comparing the peak in Me-THF (a blue shift of about 5 nm), which indicates that the lowest triplet state (T_1) of $^3(4\text{-HOPyT})^*$ has $^3(n,\pi^*)$ character.^{18,20–23} In contrast, solvent polarity does not affect the nonpolar $^3(\pi,\pi^*)$ electronic configuration of T_1 .^{18,20–23}

Transient spectra in aqueous media

In Ar-saturated buffer solution at pH 7, a transient absorption spectrum similar to Fig. 2 was observed for the 355-nm laser excitation of 4-HOPyT, suggestive of the formation of $^3(4\text{-HOPyT})^*$, 4-PyS^* and 4-S=PyO^* , which are the transient species assigned in organic solvents. To prove that the homolytic cleavage of the N–O bond of 4-HOPyT is the photoprocess that gives rise to 4-PyS^* , evidence for the concomitant formation of $\cdot\text{OH}$ was sought. Indeed, the formation of $\cdot\text{OH}$ was confirmed by an indirect method. Thus, the laser photolysis of 4-HOPyT in the presence of KSCN in Ar-saturated buffer solution at pH 7 resulted a transient absorption band with a maximum at 480 nm, which is attributed to $(\text{SCN})_2^{\cdot-}$.^{16,29} The formation of $(\text{SCN})_2^{\cdot-}$ is proposed to derive from the reaction between thiocyanate ion (SCN^-) and $\cdot\text{OH}$ according to eqn. (5a) and (5b).¹⁶ When DMSO and phenol (known as efficient



$\cdot\text{OH}$ scavengers) are added, the transient absorption band of $(\text{SCN})_2^{\cdot-}$ at 480 nm disappears.¹⁶

These observations corroborate that $\cdot\text{OH}$ is generated by the homolytic scission of the N–O bond of 4-HOPyT (Scheme 2), as previously demonstrated by spin-trapping experiments with 5,5'-dimethylpyrroline-*N*-oxide (DMPO) and subsequent EPR spectroscopy.¹⁴ In acidic buffer solution at pH 4.02, photochemical processes of 4-HOPyT similar to those at pH 7 were observed.

Fig. 5 shows the transient absorption spectra recorded by the laser photolysis ($\lambda_{\text{exc}} = 355 \text{ nm}$) of 4-HOPyT in Ar-saturated alkaline buffer solution at pH 12, in which 4-HOPyT exists as an anionic form [eqn. (6)].¹⁹ The broad band around 600 nm, which is efficiently quenched by O₂ (see inset in Fig. 5) or N₂O and decays within 10 μs in Ar-saturated solution, is assigned to solvated electron (e_{aq}^-).^{15,16,30} The absorption intensity at 680 nm did not decay completely in the presence of O₂ (see inset in Fig. 5) or N₂O due to the overlap with the absorption of 4-S=PyO^* derived from 4-HOPyT (assigned in Fig. 2 and 3) by photoionization as shown in eqn. (6).^{15,16}

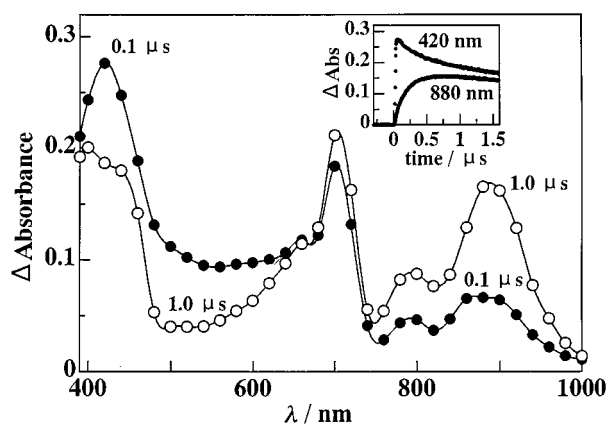
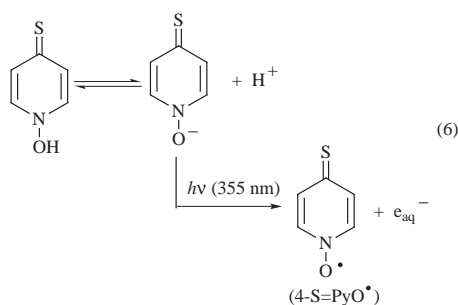


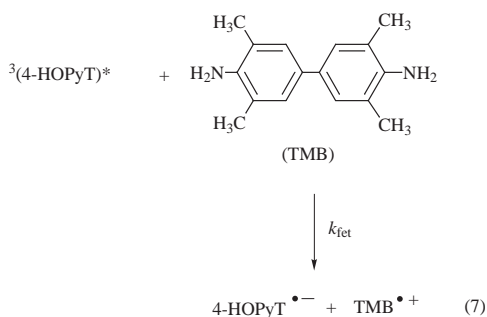
Fig. 6 Transient absorption spectra in the visible/near-IR regions of the laser photolysis of 4-HOPyT ($0.2 \times 10^{-3} \text{ mol dm}^{-3}$) at 355-nm excitation in the presence of TMB ($0.6 \times 10^{-3} \text{ mol dm}^{-3}$) in Ar-saturated acetonitrile (detector, Si-PIN). Inset: time profiles of the 420- and 880-nm absorption bands.



Photoinduced electron transfer

The transient absorption spectra of the laser photolysis (355 nm excitation light) of 4-HOPyT in the presence of tetramethylbenzidine (TMB) in Ar-saturated acetonitrile are shown in Fig. 6. The absorption maximum of $^3(4\text{-HOPyT})^*$ at 420 nm was observed immediately after the laser flash, along with the appearance of absorption bands at 800 and 880 nm due to $\text{TMB}^{\bullet+}$.^{18,31} The time profiles of the decay and the rise in the absorption of $^3(4\text{-HOPyT})^*$ and $\text{TMB}^{\bullet+}$ at 420 and 880 nm, respectively, are shown in the inset of Fig. 6. The 420-nm band of $^3(4\text{-HOPyT})^*$ did not decay completely due to its overlap with the rising absorption band of $\text{TMB}^{\bullet+}$ in the region of 400–470 nm.^{18,31}

In the presence of O_2 , the absorption of the $\text{TMB}^{\bullet+}$ was suppressed due to the quenching of $^3(4\text{-HOPyT})^*$. This finding indicates that electron transfer takes place from TMB to $^3(4\text{-HOPyT})^*$, as shown in eqn. (7),^{18,31} but not from TMB to



$^3(4\text{-PyS}^{\bullet-})$. From the rise of the $\text{TMB}^{\bullet+}$ absorption at 880 nm, the first-order rate constants (k_{fet}) were evaluated by curve-fitting with a single exponential as shown in Fig. 7. The second-order rate constant for electron transfer [k_{fet} in eqn. (7)] from TMB to $^3(4\text{-HOPyT})^*$ may be evaluated by the [TMB] dependence of

Table 2 Rate constants for forward-electron-transfer (k_{fet}) and back-electron-transfer (k_{bet}) reactions in Ar-saturated acetonitrile^a

Substrate	$k_{\text{fet}}/\text{mol}^{-1} \text{ dm}^3 \text{ s}^{-1}$	$(k_{\text{bet}}/\varepsilon_{\text{radical ion}})^b/\text{cm s}^{-1}$	$k_{\text{bet}}/\text{mol}^{-1} \text{ dm}^3 \text{ s}^{-1}$
TMB	5.5×10^9	4.9×10^5	9.9×10^9
<i>p</i> -DNB	6.6×10^9	6.9×10^5	4.1×10^9
<i>o</i> -DNB	6.1×10^9	^c	^c
<i>m</i> -DNB	5.9×10^9	^c	^c

^a Estimated error is $\pm 8\%$ of the stated values. ^b $\varepsilon_{\text{TMB}^{\bullet+}} = 20\,200 \text{ mol}^{-1} \text{ dm}^3 \text{ cm}^{-1}$ at 880 nm (Refs. 18, 31) and $\varepsilon_{p\text{-DNB}^{\bullet-}} = 5900 \text{ mol}^{-1} \text{ dm}^3 \text{ cm}^{-1}$ at 910 nm (Refs. 18, 32) in acetonitrile. ^c The transient absorption bands of *o*-DNB^{•-} and *m*-DNB^{•-} overlapped with that of $^3(4\text{-HOPyT})^*$.

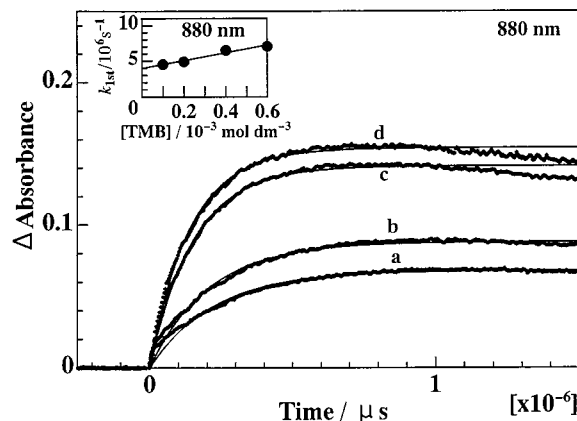


Fig. 7 Rise of the 880-nm absorption band of $\text{TMB}^{\bullet+}$ in Ar-saturated acetonitrile with [TMB]; (a) 0.1, (b) 0.2, (c) 0.4 and (d) $0.6 \times 10^{-3} \text{ mol dm}^{-3}$ (detector, Si-PIN). Inset: pseudo-first-order plot for electron transfer.

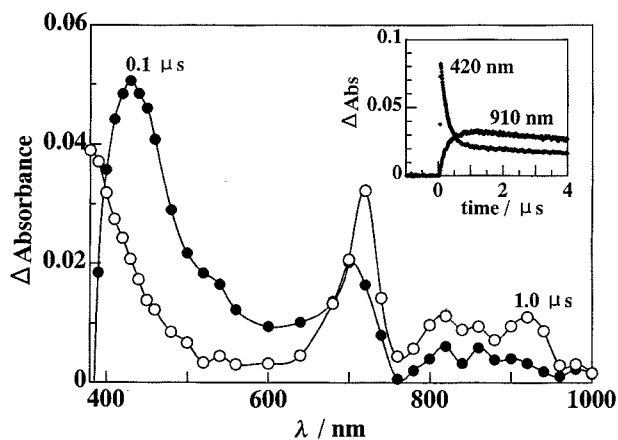


Fig. 8 Transient absorption spectra in the visible/near-IR regions of the 355-nm laser photolysis of 4-HOPyT ($0.1 \times 10^{-3} \text{ mol dm}^{-3}$) in the presence of *p*-DNB ($0.4 \times 10^{-3} \text{ mol dm}^{-3}$) in Ar-saturated acetonitrile (detector, Si-PIN). Inset: time profiles of the 420- and 910-nm absorption bands.

the first-order rate constant (see inset in Fig. 7), as listed in Table 2. The absorption band of 4-S=PyO[•] at 700 nm (Fig. 6) was not enhanced in the presence of TMB, which indicates that electron transfer does not take place between 4-S=PyO[•] and TMB.

With electron acceptors such as *p*-dinitrobenzene (*p*-DNB) in Ar-saturated acetonitrile, the absorption intensity of $^3(4\text{-HOPyT})^*$ at 420 nm decreased within a few hundred nanoseconds, new absorption bands appearing at 860 and 910 nm in the near-IR region (Fig. 8). The latter increasing absorption bands are attributed to the radical anion of *p*-DNB ($p\text{-DNB}^{\bullet-}$).^{18,32} When O_2 gas was introduced, the absorption bands for $p\text{-DNB}^{\bullet-}$ at 860 and 910 nm were suppressed, which

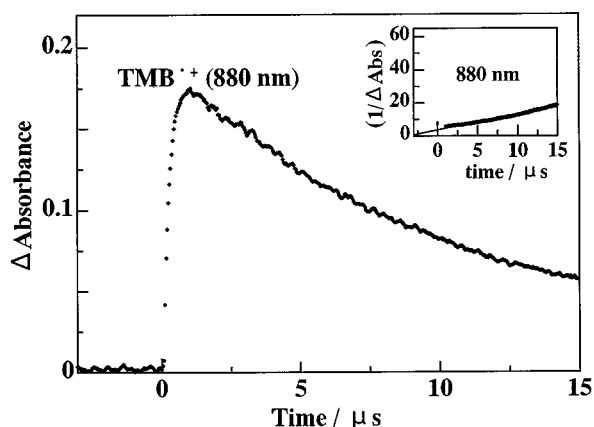
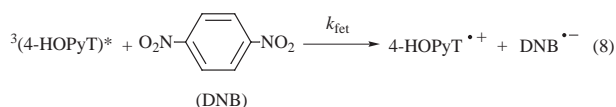


Fig. 9 Absorption-time profile at 880 nm for the decay of $\text{TMB}^{\bullet+}$ in the 355-nm laser photolysis of a mixture of TMB and 4-HOPyT in Ar-saturated acetonitrile (detector; Si-PIN). Inset: second-order plot.

indicates that $^3(4\text{-HOPyT})^*$ is the precursor for the reaction with *p*-DNB. The rate constants (k_{1st}) obtained from the decay profiles of $^3(4\text{-HOPyT})^*$ with *p*-DNB are in good agreement with those from the rise time profiles of *p*-DNB $^{\bullet-}$ absorption in acetonitrile. Thus, it is evident that the rate constants for the quenching of $^3(4\text{-HOPyT})^*$ by *p*-DNB and for the formation of *p*-DNB $^{\bullet-}$ in acetonitrile may be attributed to electron transfer (k_{fet} in Table 2) from $^3(4\text{-HOPyT})^*$ to *p*-DNB [eqn. (8)].^{18,32}



Similar results were obtained for *m*- and *o*-DNB (Table 2). These findings coincide with our previous observations that the triplet states of pyridinethiones and purinethione act as electron donors to DNB.¹⁸

The absorption intensities of the radical ions $\text{TMB}^{\bullet+}$ and $\text{DNB}^{\bullet-}$ decay slowly after reaching their maxima in acetonitrile. These decays obey second-order kinetics, as shown in Fig. 9, and may be attributed to bimolecular decay processes (k_{bd}).^{18,31,32} From the slopes of the second-order plots (see inset in Fig. 9), $k_{\text{bd}}/\epsilon_{\text{radical ion}}$ may be obtained, as listed in Table 2. By substitution of the reported values of $\epsilon_{\text{radical ion}}$,^{18,31,32} the k_{bd} values were evaluated for $\text{TMB}^{\bullet+}$ and $\text{DNB}^{\bullet-}$ in acetonitrile (Table 2). Since k_{bd} is close to k_{d} , it can be considered that the bimolecular rate constants (k_{bd}) are due to back electron transfer.

MO calculations

The unpaired π -electron densities of the SOMO and the electronic transition energies of 4-PyS $^{\bullet}$ and 4-S=PyO $^{\bullet}$ were calculated by the unrestricted open-shell Hartree-Fock (ROHF) method on the geometries optimized at the MNDO/CI level by using the MOPAC program package.³³ The unpaired π -electron is mainly localized on the S atom in 4-PyS $^{\bullet}$. In the case of 4-S=PyO $^{\bullet}$, the unpaired π -electron density on the O atom is greater than on the other atoms. The first allowed electronic transitions of 4-PyS $^{\bullet}$ and 4-S=PyO $^{\bullet}$ were calculated to be 430 (oscillator strength = 0.54) and 725 (oscillator strength = 0.68) nm, respectively, which are in good agreement with the observed λ_{max} at 420 and 710 nm, respectively. Thus, the MO calculations substantiate the experimental assignments of the 4-PyS $^{\bullet}$ and 4-S=PyO $^{\bullet}$ radical species.

Concluding remarks

In the present study, it has been disclosed that the photochemistry of 4-HOPyT is rather complicated; 4-PyS $^{\bullet}$ and $\cdot\text{OH}$ were generated by homolytic N–OH bond cleavage concomi-

tant with the formation of $^3(4\text{-HOPyT})^*$. 4-S=PyO $^{\bullet}$ was produced by direct photodissociation of the O–H bond as well as by the reactions of $^3(4\text{-HOPyT})^*$ and $\cdot\text{OH}$ with 4-HOPyT. In aqueous alkaline solution, solvated electron (e_{aq}^-) and 4-S=PyO $^{\bullet}$ were produced by photoionization of the anionic form of 4-HOPyT. Thus, the change of pH allows control of the generation of $\cdot\text{OH}$.

The lowest triplet-state energy (E_{T}) of $^3(4\text{-HOPyT})^*$ was evaluated as 60.1 kcal mol $^{-1}$. From the polar nature of $^3(4\text{-HOPyT})^*$, the electronic configuration of T_1 is attributed to $^3(n,\pi^*)$. The high triplet energy of $^3(4\text{-HOPyT})^*$ may be related to the electron donor-acceptor properties of $^3(4\text{-HOPyT})^*$ with the electron acceptor DNB and the electron donor TMB in polar solvents.

Experimental

Materials and methods

N-Hydroxypyridine-4-thione (4-HOPyT) was prepared by the method described elsewhere.^{19,34} Commercially available 4,4'-dipyridine disulfide (DPDS), 3,3',5,5'-tetramethylbenzidine (TMB), dinitrobenzenes (DNB's) and other reagents were used after recrystallization. 1,3-Diphenylisobenzofuran (DPBF) and β -carotene were purchased from the Aldrich Chemical Co. Solvents used for the transient absorption measurements were of spectroscopic grade. Absorption and fluorescence spectra were determined on UV-VIS (Jasco V-570) and fluorescence (Shimadzu RF-5300PC) spectrophotometers with an appropriate optical path. The phosphorescence spectrum was measured in frozen glassy media at 77 K.

The laser-flash-photolysis apparatus was a standard design equipped with Nd:YAG laser (fwhm 6 ns).^{18,24} The solutions were photolyzed at 355 nm from a third-harmonic generator (THG). Transient spectra were recorded with a multichannel photodiode (MCPD) system. The time profiles in the visible region were followed by a photomultiplier tube (PMT) as a detector during continuous irradiation with a Xe lamp (150 W). In the visible and near-IR regions (350–1000 nm), an Si-PIN photodiode attached to a monochromator was also employed as a detector to monitor the probe light from a pulsed xenon-flash lamp. The output signal from the detector was recorded with a digitizing oscilloscope and processed by means of a personal computer.^{18,24} The laser photolysis was performed at 23 °C for deaerated and O $_2$ -saturated solutions, obtained by purging with Ar and O $_2$ gas, respectively, in a rectangular quartz cell with a 10-mm optical path.

MO calculations

The MO calculations were performed by the MNDO method by using MOPAC, available from the Japan Program Exchange Association.³³

Acknowledgements

The authors from Sendai would like to thank Drs A. Watanabe and M. Fujitsuka (Tohoku University) for their comments. The authors from Würzburg appreciate generous financial support from the Deutsche Forschungsgemeinschaft (Sonderforschungsbereich 172 "Molekulare Mechanismen kanzerogener Primärveränderungen") and the Fonds der Chemischen Industrie.

References

- 1 E. Shaw, J. Bernstein, K. Loser and W. A. Lott, *J. Am. Chem. Soc.*, 1950, **72**, 4362.
- 2 D. H. R. Barton, D. Crich and W. B. Motherwell, *Tetrahedron*, 1985, **41**, 3901.
- 3 D. H. R. Barton and S. Z. Zard, *Pure Appl. Chem.*, 1986, **58**, 675.
- 4 M. Newcomb and U. Park, *J. Am. Chem. Soc.*, 1986, **108**, 4132.

- 5 M. Newcomb and J. Kaplan, *Tetrahedron Lett.*, 1987, **28**, 1615.
- 6 J. Boivin, E. Crepon and S. Z. Zard, *Tetrahedron Lett.*, 1990, **31**, 6869.
- 7 A. Albert, *Selective Toxicity: The Physico-Chemical Basis of Therapy*, 7th edn., Chapman and Hall, London, 1985.
- 8 G. J. Kontoghiorghes, A. Piga and A. V. Hoffbrand, *Hematol. Oncol.*, 1986, **4**, 195.
- 9 J. Blatt, S. R. Taylor and G. J. Kontoghiorghes, *Cancer Res.*, 1989, **49**, 2925.
- 10 W. Adam, J. Cadet, F. Dall'Acqua, D. Ramaiah and C. R. Saha-Moeller, *Angew. Chem.*, 1995, **107**, 91.
- 11 N. J. Van Abbe, P. M. Baxter, J. J. Jackson, M. A. Bell and H. Dixon, *Int. J. Cosmetic Sci.*, 1981, **3**, 233.
- 12 D. H. R. Barton, J. C. Jaszberenyi and A. I. Morrell, *Tetrahedron Lett.*, 1991, **32**, 311.
- 13 K. M. Hess and T. A. Dix, *Anal. Biochem.*, 1992, **206**, 309.
- 14 W. Adam, D. Ballmaier, B. Epe, G. N. Grimm and C. R. Saha-Moeller, *Angew. Chem., Int. Ed. Engl.*, 1995, **34**, 2156.
- 15 M. M. Alam, A. Watanabe and O. Ito, *Photochem. Photobiol.*, 1996, **63**, 53.
- 16 (a) B. M. Aveline, I. E. Kochevar and R. W. Redmond, *J. Am. Chem. Soc.*, 1996, **118**, 289; (b) B. M. Aveline, I. E. Kochevar and R. W. Redmond, *J. Am. Chem. Soc.*, 1996, **118**, 10 113.
- 17 B. Epe, D. Ballmaier, W. Adam, G. N. Grimm and C. R. Saha-Moeller, *Nucleic Acids Res.*, 1996, **24**, 1625.
- 18 (a) M. M. Alam, M. Fujitsuka, A. Watanabe and O. Ito, *J. Phys. Chem. A*, 1998, **102**, 1338; (b) M. M. Alam, M. Fujitsuka, A. Watanabe and O. Ito, *J. Chem. Soc., Perkin Trans. 2*, 1998, 817.
- 19 R. A. Jones and A. R. Katritzky, *J. Chem. Soc.*, 1960, 2937.
- 20 J. Wirz, *J. Chem. Soc., Perkin Trans. 2*, 1973, 1307.
- 21 (a) A. Maciejewski, D. R. Demmer, D. R. James, A. Safarzadeh-Amiri, R. E. Verrall and R. P. Steer, *J. Am. Chem. Soc.*, 1985, **107**, 2831; (b) A. Maciejewski, M. Syzmanski and R. P. Steer, *J. Phys. Chem.*, 1988, **92**, 6939.
- 22 V. Ramamurthy and R. P. Steer, *Acc. Chem. Res.*, 1988, **21**, 380.
- 23 A. Maciejewski and R. P. Steer, *Chem. Rev.*, 1993, **93**, 67.
- 24 (a) M. M. Alam, A. Watanabe and O. Ito, *J. Org. Chem.*, 1995, **60**, 3440; (b) M. M. Alam, H. Konami, A. Watanabe and O. Ito, *J. Chem. Soc., Perkin Trans. 2*, 1996, 263; (c) M. M. Alam and O. Ito, *Recent Res. Dev. Photochem. Photobiol.*, 1997, **1**, 51.
- 25 C. Chatgililoglu and K.-D. Asmus, *Sulfur-Centered Reactive Intermediates in Chemistry and Biology*, NATO ASI Series A: Life and Science vol. 197, Plenum Press, New York, 1990, pp. 327–340.
- 26 H. H. Wasserman and R. W. Murray, in *Singlet Oxygen*, Academic Press, New York, 1979, ch. 5, 6, 8 and 9.
- 27 (a) S. L. Murov, *Handbook of Photochemistry*, Marcel Dekker, New York, 1973; (b) A. Farmilo and F. Wilkinson, *Chem. Phys. Lett.*, 1975, **34**, 495; (c) C. Lambert and R. W. Redmond, *Chem. Phys. Lett.*, 1994, **228**, 495.
- 28 K. Sandros, *Acta Chem. Scand.*, 1964, **18**, 2355.
- 29 D. H. Ellison, G. A. Salmon and F. Wilkinson, *Proc. R. Soc. London, Ser. A*, 1972, **328**, 23.
- 30 J. H. Edwin, *Solvated Electron: Advances in Chemistry Series*, American Chemical Society, Washington, DC, 1965, pp. 37–40.
- 31 (a) A. Watanabe, O. Ito and K. Mori, *Synth. Met.*, 1989, **32**, 237; (b) Y. Sasaki, Y. Yoshikawa, A. Watanabe and O. Ito, *J. Chem. Soc., Faraday Trans.*, 1995, **91**, 2287.
- 32 (a) M. Fujitsuka, T. Sato, T. Shimidzu, A. Watanabe and O. Ito, *J. Phys. Chem. A*, 1997, **101**, 1056; (b) T. Shida, *Electronic Absorption Spectra of Radical Ions*, Physical Science data 34, Elsevier, Amsterdam, 1988.
- 33 (a) J. J. P. Stewart, *J. Comput. Chem.*, 1989, **10**, 209; (b) J. J. P. Stewart, *Quantum Chemistry Program Exchange Bull.*, 1989, **9**, 10.
- 34 (a) E. Ochiai, *J. Org. Chem.*, 1953, **18**, 543; (b) D. H. R. Barton, D. Crich, and G. Kretzschmar, *J. Chem. Soc., Perkin Trans. 1*, 1986, 39.

Paper 8/04592E